Redox Transformations at Nanodiamond Surfaces Revealed by *in situ* Infrared Spectroscopy

Jan Scholz[a] , A. James McQuillan[a] and Katherine B. Holt[*b]

Electronic Supporting Information

1. Characterisation of Nanodiamond (ND) and preparation of ND-modified electrode.

Nanodiamond (ND) powder was obtained commercially from Shenzhen Jingangyuan New Material Company, P.R. China and was used as received. This material has previously been characterised using XPS, Raman and IR spectroscopy and its electrochemical properties previously reported [ESI1].

For all experiments a commercial highly doped boron-doped diamond (BDD) electrode (Windsor Scientific, UK) of 3 mm diameter was used, as BDD has a low current and featureless background response making it ideal for experiments requiring high sensitivity towards low concentrations of analyte. A platinum mesh was used as the counter electrode and a Ag / AgCl electrode as the reference. Experiments were carried out using an Autolab PGSTAT10 potentiostat (Ecochemie) with GPES software. To produce the ND-modified electrodes, a known volume of ND suspended in Analar ethanol was drop-coated onto the BDD electrode and allowed to dry. The drop-coated layer was extremely stable and remained on the surface of the electrode even after long times in aqueous solution.

The initial suspension of ND was made up of 0.5 ± 0.05 mg ND powder in 1.5 ± 0.2 mL of ethanol, which was vortex mixed and then sonicated for 20 minutes prior to use. It is known that ND forms aggregates in solution of several 100 nm in diameter and it is difficult to produce a deagglomerated suspension of individual 5 nm nanoparticles [ESI2]. Apart from the sonication no further attempt was made to break up the aggregates and so it is very likely that our ND suspension and drop-coated layer consists of aggregates of the particles.

2. Cyclic Voltammetry (CV) of ND-modified electrode

The ND-modified electrode was cycled repeatedly (20 scans) in 0.1 M NaCl solution at 10 mV s^{-1} (first 5 scans shown in Fig ES1).

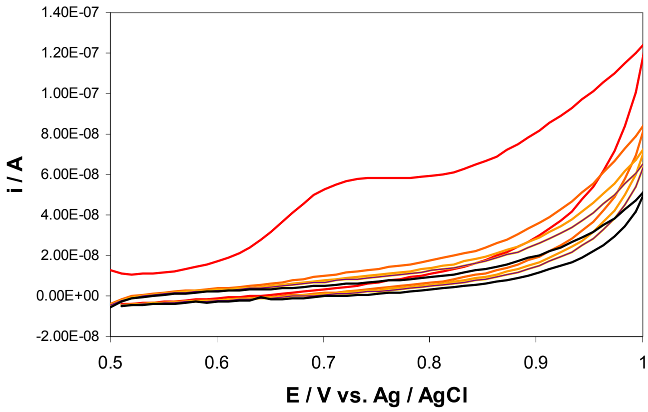

Figure ES1: *First 5 consecutive CVs for ND-modified BDD electrode in 0.1 M NaCl at 10 mV s*$^{-1}$ *(scan 1: red; scan 2: dark orange; scan 3: light orange; scan 4: yellow; scan 5: brown; scans 4 and 5 and subsequent scans are almost identical). Also shown is the background scan of clean BDD electrode under same conditions.*

Only the voltammetric activity of the ND in the potential range 0.5 V to 1 V was investigated in this study, as this is the region of interest for its interaction with the $IrCl_6^{3-/2-}$ couple. However the ND does undergo oxidation and reduction at lower potentials, which have been reported in some detail previously [ESI1, ref 5 in main text].

A freshly prepared ND-modified electrode was also cycled repeatedly (20 scans) in 1 µM $IrCl_6^{3-}$ in 0.1 M NaCl solution at 10 mV s^{-1} (first 5 scans shown in Fig ES2).

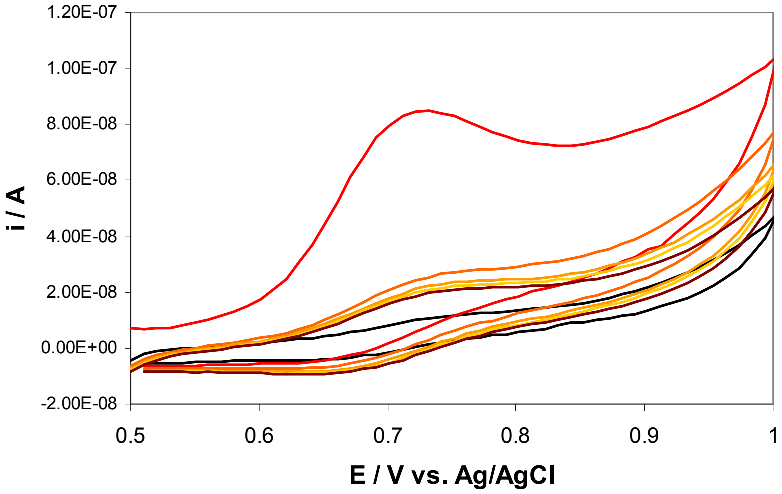

Figure ES2: *First 5 consecutive CVs for ND-modified BDD electrode in 1 µM $IrCl_6^{3-}$ in 0.1 M NaCl at 10 mV s^{-1} (scan 1: red; scan 2: dark orange; scan 3: light orange; scan 4: yellow; scan 5: brown). Also shown is the background scan of clean BDD electrode under same conditions.*

The charge passed during the forward scan for each of these CVs was calculated by integration using the GPES software analytical tools. Fig 1 b in the main document shows a plot of the charge passed in the CVs in Fig ES2 minus the charge passed for the corresponding CV in Fig ES1.

3. IR analysis of ND particle films

A FTIR spectrometer (Digilab, FTS 4000) equipped with a Peltier-cooled DTGS detector and purged with dried air was used. Spectra were collected from 16 co-added scans at 4 cm^{-1} resolution using a diamond-faced triple-reflection ZnSe ATR prism (DuraSamplIR, ASI SensIR Techn.) in the spectral range from 3800 to 850 cm^{-1} from 256 co-added scans (IR spectrum of the ND particle film in Fig 2) and 64 co-added scans (IR spectra collected upon $[IrCl_6]^{2-}$ contact in Fig 3) with a spectral resolution of 4 cm^{-1}. The spectral range between 2700 and 1800 cm^{-1} was omitted in Fig 1 due to cut-out of the diamond ATR-IR prism. Resolution Pro 4.0 (Digilab) and OPUS 6.0.72 (Bruker) software packages have been used for data evaluation. Figures containing IR spectra were made using OriginPro 8 software package (OriginLab).

3.1 Identification of spectral components of the ND particle film

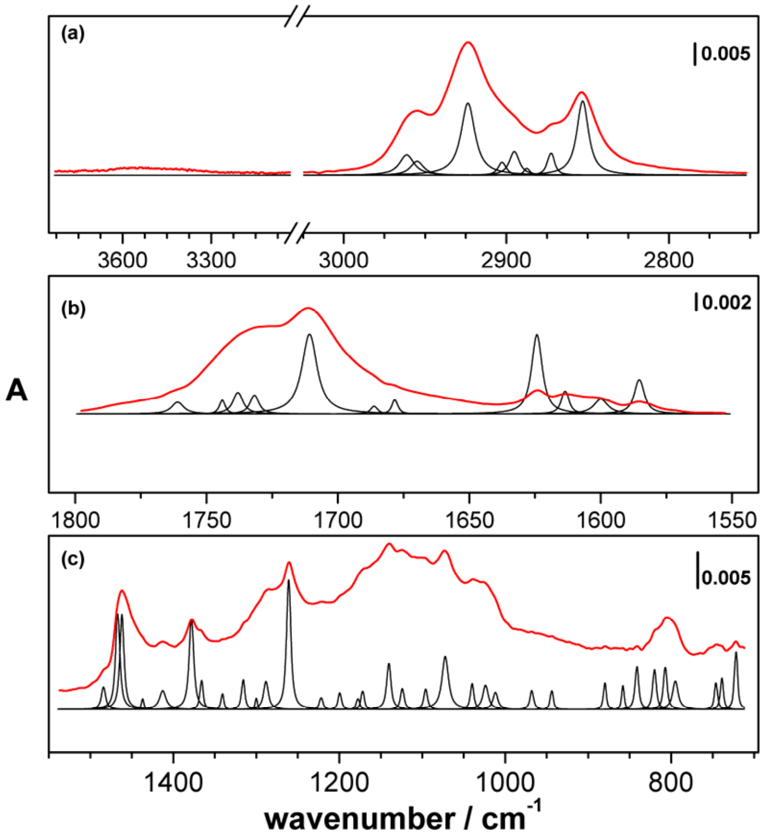

Figure ES3: *IR absorption spectrum of dry ND film from Fig. 2 (red line) and its spectral component bands (black lines).*

Individual absorptions contributing to the IR spectra of ND material in Fig 2 were identified from the analysis of second derivative spectra of the dry ND particle film followed by peak deconvolution studies (not shown). Second derivative spectra for three different ND particle films were generated using mentioned software package. Those absorptions present in all three second derivative spectra were submitted to peak deconvolution studies of the ND film spectrum (red line) in three spectral ranges (Fig. ES3a-c). The absorbance values observed for deconvoluted component bands were checked against S/N ratio of ND spectrum (absorbance threshold), and only those deconvoluted absorptions meeting the threshold were considered spectral contributions to the ND film spectrum in Fig. 2. In Figure ES3a-c all second derivative absorptions meeting the absorbance threshold in the deconvolution study are given as individual peaks (black line). Peak intensities are arbitrary.

3.2 IR Difference spectrum of 3800 – 2600 cm^{-1} region

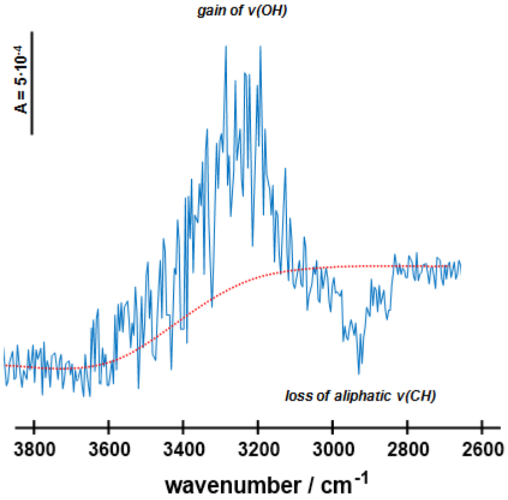

Figure ES4: *IR difference absorption spectra of ND film after 2 h contact with 10 µM* $IrCl_6^{2-}$ *(0.1 M NaCl, pH 4, Ar) vs. ND film in (0.1 M NaCl, pH 4, Ar) in the 3900-2600 cm*$^{-1}$ *spectral range. Baseline trend is indicated by red dotted line.*

Spectral change of νOH and νCH related absorptions upon 2 h of $IrCl_6^{2-}$ contact with ND particle film indicating absorbance losses about 2970, 2920 and 2850 cm^{-1} accounting for circa 1% of the respective absorbance in Figure 2, which are ascribed to modes of aliphatic $CH/CH_2/CH_3$ surface groups affected upon $IrCl_6^{2-}$ contact. Evidence for equally intense arylic νCH modes is lacking. The minor absorbance gain about 3200 cm^{-1} is attributed to surface-bound water (H-bonding) [ESI3]. Absorbance changes of features for this spectral range were not considered in the quantitative (Fig. 4) and temporal analysis (Fig. 5) due to insufficient signal-to-noise, reflecting the reduced spectral sensitivity at higher wavenumber typical for the ATR approach [ESI4].

3.3 IR difference spectrum in absence of oxidant $IrCl_6^{2-}$

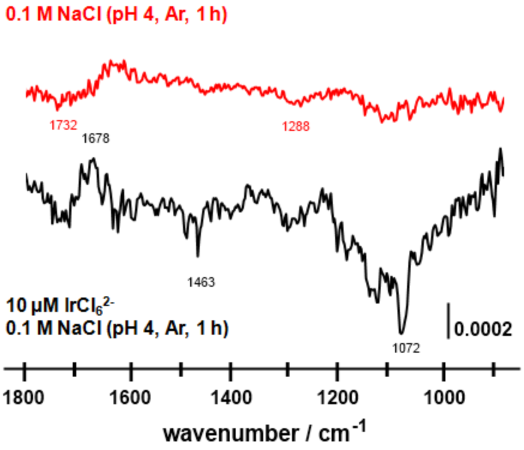

Figure ES4: *Comparison of the spectral changes in the presence and absence of* $IrCl_6^{2-}$ *after 1 h.*

The comparison of the IR spectra of a ND particle film in contact with an acidic electrolyte both in the presence (black spectrum) and absence of $IrCl_6^{2-}$ (red spectrum) clearly unveils the effect of the oxidant on ND surface functional groups. Prominent absorbance loss and gain features occurring in the presence of $IrCl_6^{2-}$, e.g. at 1678, 1463 or 1072 cm^{-1}, were not reproduced in its absence. Loss features about 1732 and 1288 cm^{-1} evident in both spectra may refer to an underlying reaction of ND surface functional groups in the presence of the background electrolyte. Acid catalysed condensation and/or decarboxylation reactions have been suggested in the text.

References

[ESI1] K. B. Holt, C. Ziegler, D. J. Caruana, J. B. Zang, E. J. Millán-Barrios, J. P.Hu, J. S. Foord, *Phys. Chem. Chem. Phys.*, 2008, **10**, 303.
[ESI2] A. Krueger, F. Kataoka, M. Ozawa, M. Fujino, T. Suzuki, Y. Aleksenskii, A. E. Vul', A. Ya, E. Osawa, *Carbon,* 2005, **43**, 1722.
[ESI3] Nakamoto, K. Infrared and Raman Spectra of Inorganic and Coordination Compounds: John Wiley & Sons, Inc.: New Jersey, 2009.
[ESI4] Harrick, N.J. *Internal Reflection Spectroscopy*. John Wiley & Sons Inc, 1967.